



HHS Public Access

Author manuscript

Nat Neurosci. Author manuscript; available in PMC 2014 April 01.

Published in final edited form as:

Nat Neurosci. 2013 October ; 16(10): 1417–1425. doi:10.1038/nn.3516.

Synapse Maturation by Activity-Dependent Ectodomain Shedding of SIRP α

Anna B. Toth^{1,4}, Akiko Terauchi^{1,4}, Lily Y. Zhang^{1,4}, Erin M. Johnson-Venkatesh^{1,4}, David J. Larsen¹, Michael A. Sutton^{1,2}, and Hisashi Umemori^{1,3,*}

¹Molecular & Behavioral Neuroscience Institute, University of Michigan Medical School, Ann Arbor, MI 48109-2200

²Department of Molecular and Integrative Physiology, University of Michigan Medical School, Ann Arbor, MI 48109-2200

³Department of Biological Chemistry, University of Michigan Medical School, Ann Arbor, MI 48109-2200

Abstract

Formation of appropriate synaptic connections is critical for proper functioning of the brain. After initial synaptic differentiation, active synapses are stabilized by neural activity-dependent signals to establish functional synaptic connections. However, the molecular mechanisms underlying activity-dependent synapse maturation remain to be elucidated. Here we show that activity-dependent ectodomain shedding of SIRP α mediates presynaptic maturation. Two target-derived molecules, FGF22 and SIRP α , sequentially organize the glutamatergic presynaptic terminals during the initial synaptic differentiation and synapse maturation stages, respectively, in the mouse hippocampus. SIRP α drives presynaptic maturation in an activity-dependent fashion. Remarkably, neural activity cleaves the extracellular domain of SIRP α , and the shed ectodomain, in turn, promotes the maturation of the presynaptic terminal. This process involves CaM kinase, matrix metalloproteinases, and the presynaptic receptor CD47. Finally, SIRP α -dependent synapse maturation has significant impacts on synaptic function and plasticity. Thus, ectodomain shedding of SIRP α is an activity-dependent trans-synaptic mechanism for the maturation of functional synapses.

Users may view, print, copy, download and text and data- mine the content in such documents, for the purposes of academic research, subject always to the full Conditions of use: http://www.nature.com/authors/editorial_policies/license.html#terms

*To whom correspondence should be addressed. Hisashi Umemori, Molecular & Behavioral Neuroscience Institute and Department of Biological Chemistry, University of Michigan Medical School, Room 5065, BSRB, 109 Zina Pitcher Place, Ann Arbor, MI 48109-2200, Phone: 734-763-5242, Fax: 734-936-2690, umemoh@umich.edu or hisashi.umemori@childrens.harvard.edu.

⁴These authors contributed equally to this work.

Note: Supplementary information is available on the Nature Neuroscience website.

AUTHOR CONTRIBUTIONS

H.U. designed experiments and prepared the manuscript. A.B.T., A.T., L.Y.Z., E.M.J.V., and D.J.L. performed experiments. M.A.S. and H.U. supervised the project. All authors analyzed data and commented on the manuscript.

COMPETING FINANCIAL INTERESTS

The authors declare no competing financial interests.

INTRODUCTION

Synapses are the sites of information processing between neurons in the brain. Defects in synaptic circuitry in the hippocampus, a structure critical for long-term memory formation, emotional processing and social behavior, are associated with a variety of neurological and psychiatric disorders including Fragile X syndrome, autism, epilepsy, and schizophrenia¹⁻³. Thus, proper assembly of hippocampal synapses is essential for optimal functioning of the brain. To organize synapse formation, signals are exchanged between pre- and postsynaptic neurons. Two forms of signals are required for functional synapse formation during development: activity-independent and activity-dependent signals. Usually, initial synaptic differentiation is regarded as activity-independent steps, whereas a period of activity-dependent synapse maturation shapes the ultimate structure of neural circuits⁴⁻⁷. During synapse maturation, activity-dependent signals either stabilize or eliminate axons and further mature selected synapses to establish appropriate synaptic connections⁸⁻¹². Thus, activity-dependent mechanisms are required for the structural refinement of neural circuits, to match pre- and postsynaptic function, and for the final arrangement of the appropriate synaptic map¹¹⁻¹⁴. While synapse stabilization/destabilization and maturation are clearly activity-dependent, little is known about molecular mechanisms underlying them. Defects in activity-dependent synapse maturation in the hippocampus have been implicated in various neurodevelopmental disorders, including schizophrenia and autism¹⁻³. Therefore, the understanding of the molecules and manner by which hippocampal circuits are established by neural activity should yield novel insights into both the etiology and treatment of these devastating disorders.

To understand the molecular mechanisms of synapse formation, we have performed an unbiased search for molecules that promote differentiation of axons into presynaptic nerve terminals. Using the ability to cluster synaptic vesicles in cultured motor neurons as a bioassay, we have purified molecules that can promote differentiation of axons into presynaptic nerve terminals from developing brains and identified two molecules, FGF22 (fibroblast growth factor 22)¹⁵ and SIRP α (signal regulatory protein α)¹⁶, as such presynaptic organizers. We have shown that FGF22 and its close relative FGF7 are selectively involved in the initial organization of excitatory (glutamatergic) and inhibitory (GABAergic) synapses, respectively, in the hippocampus¹⁷. The other molecule, SIRP α , is a transmembrane immunoglobulin superfamily member that is involved in various hematopoietic cell functions¹⁸⁻²⁰, but little is known about its roles in the brain. We therefore investigated the role, mechanism, and impact of SIRP α -dependent synapse formation in the brain.

Here we show that: 1) Target-derived molecules FGF22 and SIRP α sequentially organize presynaptic terminals; 2) SIRP α is necessary for presynaptic maturation, but not for induction or maintenance, in the hippocampus *in vivo*; 3) SIRP α drives presynaptic maturation in an activity-dependent manner; 4) Activity cleaves the ectodomain of SIRP α , and this cleavage is required for SIRP α 's presynaptic effects; 5) Calcium, calcium/calmodulin-dependent protein kinase (CaMK) and matrix metalloproteinase (MMP) mediate SIRP α cleavage; 6) CD47 is SIRP α 's presynaptic receptor; and 7) SIRP α has a significant impact on synaptic function and plasticity. These results indicate that ectodomain shedding

of SIRP α is an activity-dependent mechanism allowing pre- and postsynaptic terminals to communicate for the maturation of functional synapses.

RESULTS

Distinct expression of FGF and SIRP α during synaptogenesis

We first compared the expression patterns of SIRP α and FGFs in the hippocampus during synapse formation. *In situ* hybridization experiments with mouse brain sections showed little *Sirpa* mRNA expression in hippocampal neurons at postnatal day 8 (P8; Fig. 1a), an early stage of synapse formation^{21,22}, but substantially higher expression at P21, a late stage of synapse formation. Western blotting confirmed a robust increase in the amount of SIRP α proteins from P8 to P21 (Fig. 1b). This expression pattern is in contrast to the patterns of *Fgf22* and *Fgf7* mRNA, which were highly expressed at P8¹⁷, but not at P21 (Supplementary Fig. 1). These results suggest that FGFs and SIRP α are involved in the early and late stages of synapse formation, respectively, in the hippocampus.

We next examined the localization of SIRP α in hippocampal neurons. Biochemical fractionation experiments revealed that SIRP α is abundant in the synaptic membrane fraction, indicating that SIRP α is a synaptic molecule. Notably, it was most enriched in the extra-junctional fraction (Supplementary Fig. 2), which is similar to some of other synaptogenic molecules including EphB2²³. Immunostaining of cultured hippocampal neurons showed that SIRP α was preferentially localized at MAP2-positive dendrites relative to neurofilament-positive axons (Fig. 1c). In dendrites, SIRP α was concentrated at excitatory synapses: it was co-localized (~75%) with vesicular glutamate transporter 1 (VGLUT1), a marker for glutamatergic presynaptic terminals, but showed little co-localization (~13%) with vesicular GABA transporter (VGAT), a marker for GABAergic presynaptic terminals (Fig. 1d). These results suggest that SIRP α is localized in dendrites at glutamatergic synapses (i.e., postsynaptic) and may serve as a target-derived glutamatergic presynaptic organizer in the hippocampus.

SIRP α promotes glutamatergic presynaptic differentiation

To address whether SIRP α can promote presynaptic differentiation of hippocampal neurons, we examined the effect that SIRP α has on synaptic vesicle clustering using a co-culture system²⁴, where neurons are co-cultured with HEK cells. The number and size of synapsin puncta formed on HEK cells expressing SIRP α were significantly larger than those on control HEK cells (Fig. 1e). SIRP α 's presynaptic effects were comparable to those of neuroligin1, a well-characterized synaptogenic molecule, indicating that SIRP α is a synaptogenic molecule that can promote synaptic vesicle clustering in hippocampal neurons.

We then examined whether SIRP α can organize glutamatergic presynaptic differentiation. For this, we prepared the extracellular portion of SIRP α ¹⁶ (soluble SIRP α – sSIRP α) and bath-applied it (2 nM) to the media of cultured hippocampal neurons for 10 days. sSIRP α significantly increased the number and size of VGLUT1 puncta (Fig. 1f). Furthermore, SIRP α increased the number and size of bassoon puncta, suggesting that SIRP α organizes active zones as well (Supplementary Fig. 3a). Electrophysiological recordings indicated that

sSIRP α increased the frequency, but not the amplitude, of miniature excitatory postsynaptic currents (mEPSCs; Fig. 1g), consistent with an increase in synaptic contacts. sSIRP α did not significantly affect dendrite/axon differentiation or the clustering of PSD95, a postsynaptic scaffolding protein at glutamatergic synapses (Supplementary Fig. 3b,c), but did increase the colocalization between VGLUT1 and PSD95 (Supplementary Fig. 3c). These results indicate that SIRP α can specifically promote presynaptic differentiation of glutamatergic synapses in hippocampal neurons.

FGF22 and SIRP α promote distinct stages of synaptogenesis

Based on the developmentally different expression of *Fgf22* and *Sirpa* mRNAs in the hippocampus, we hypothesized that FGF22 and SIRP α are preferentially involved in the early and late stages of glutamatergic synapse formation, respectively. To test this idea, we performed time course experiments using cultured hippocampal neurons. In our hippocampal cultures, glutamatergic synapse formation starts around days in vitro (DIV) 3 and slows down around DIV12¹⁷. To determine the time during which FGF22 and SIRP α are most effective at promoting presynaptic differentiation, we cultured hippocampal neurons and applied recombinant FGF22 or sSIRP α during three different periods: DIV1–DIV4, DIV4–DIV8, or DIV8–DIV11, which corresponds to the beginning, middle, and ending of synapse formation, respectively (Fig. 1h). All cultures were stained for VGLUT1 at DIV11. We found that FGF22 treatment was most effective at increasing the number and size of VGLUT1 puncta when applied from DIV1–4 (Fig. 1i,j and Supplementary Fig. 4), consistent with an early role in synapse development. In contrast, sSIRP α treatment increased the number and size of VGLUT1 puncta most prominently when it was applied from DIV8–11. These results support the notion that FGF22 and SIRP α are presynaptic organizing molecules with temporally distinct roles during synapse formation, with FGF22 in early and SIRP α in late stages of synapse formation.

To further show that FGF22 and SIRP α have distinct roles in presynaptic differentiation, we cultured FGF22-deficient neurons¹⁷ and examined whether SIRP α can rescue their synaptic defects. There were fewer and smaller VGLUT1 puncta on CA3 neurons in FGF22-deficient cultures relative to wild type cultures. These presynaptic defects were rescued by the application of FGF22, but not by SIRP α , to cultures (Fig. 1k). These results suggest that although both FGF22 and SIRP α can induce presynaptic differentiation, their specific roles in presynaptic differentiation are different.

SIRP α is required for presynaptic maturation *in vivo*

In FGF22^{-/-} mice, the differentiation of glutamatergic nerve terminals in the hippocampus is impaired early in synapse development at P8¹⁷. To identify the developmental stages during which SIRP α is critical for synapse formation *in vivo*, we generated a conditional SIRP α knockout mouse (Supplementary Fig. 5a). To temporally control the expression of SIRP α , floxed SIRP α mice were mated with actin-Cre-ER mice²⁵ and injected with tamoxifen at different postnatal days to induce Cre-mediated excision of the *Sirpa* gene. Tamoxifen injections effectively inactivated SIRP α in the hippocampus of these mice as confirmed by immunostaining for SIRP α (Supplementary Fig. 5b). In the rodent hippocampus, synapse formation starts in the first postnatal week^{21,22}. After their initial

formation, synapses are then refined in an activity-dependent manner: effective synapses are stabilized and mature, while inactive contacts are destabilized and eliminated^{4–10}. We have previously shown that activity-dependent synapse refinement in the hippocampus occurs between P15 and P25²⁶. Thus, we chose three time periods corresponding to three different stages of synapse development to inactivate SIRP α : P0–P14 (initial synapse differentiation); P15–P29 (synapse maturation); and P30–P44 (synapse maintenance). When we injected SIRP α conditional knockout mice with tamoxifen at P0 and stained their hippocampi for VGLUT1 at P14, the intensity of VGLUT1 staining was not significantly different in the SIRP $\alpha^{-/-}$ mice as compared to control (Fig. 2a), indicating that contrary to FGF22¹⁷, SIRP α is not critical for initial synapse development. In contrast, when we injected tamoxifen at P15 and analyzed at P29, the intensity of VGLUT1 staining was significantly reduced in the knockout hippocampus as compared to controls (Fig. 2b). Further analyses revealed that the size and intensity of each VGLUT1 punctum were decreased in SIRP $\alpha^{-/-}$ mice. In addition to VGLUT1, the intensity of bassoon staining, a marker for active zones, was also decreased in the knockout mice relative to control mice (Fig. 2c). These results suggest that SIRP α inactivation significantly affects the maturation of presynaptic terminals. Finally, when we injected tamoxifen at P30 and analyzed at P44, the intensity of VGLUT1 staining was not significantly different in the knockout mice as compared to control (Fig. 2d). These results demonstrate that SIRP α is critical for presynaptic maturation (P15–P29) but is not necessary for initial synapse development or synapse maintenance *in vivo*.

We also performed a series of experiments to examine whether the inactivation of SIRP α primarily affects presynaptic maturation. In the SIRP $\alpha^{-/-}$ mice with tamoxifen injected at P15, the hippocampus looked anatomically normal, and the fate of the cells in the hippocampus appeared to be unchanged (Supplementary Fig. 6a–d). In addition, the clustering of PSD95 was not significantly decreased in SIRP $\alpha^{-/-}$ as compared to control mice (Supplementary Fig. 6e). Thus, SIRP α appears to be primarily involved in presynaptic maturation in the hippocampus *in vivo*. Consistent with its expression pattern (Fig. 1a and data not shown), presynaptic maturation in SIRP $\alpha^{-/-}$ mice was impaired throughout the hippocampus (Supplementary Fig. 6f), as well as in the cerebellum. The presynaptic defects in SIRP $\alpha^{-/-}$ mice were still detected at P130 (Supplementary Fig. 6g), suggesting that SIRP α inactivation prevents presynaptic maturation rather than just delaying it.

To further confirm the role of SIRP α in presynaptic maturation, we examined the ultrastructure of excitatory (asymmetric) synapses formed in the hippocampus in P29 SIRP $\alpha^{-/-}$ mice injected with tamoxifen at P15 (Fig. 2e). We found significantly fewer synaptic vesicles and fewer docked synaptic vesicles in the asymmetric synapse in SIRP $\alpha^{-/-}$ mice relative to control. In addition, the shape of synaptic vesicles in SIRP $\alpha^{-/-}$ mice looked irregular compared to control.

Diminished transmitter release probability in SIRP $\alpha^{-/-}$ mice

To directly address the functional state of synapses in SIRP $\alpha^{-/-}$ mice, we recorded evoked field excitatory postsynaptic potentials (fEPSPs) at CA3-CA1 synapses in acute hippocampal slices (tamoxifen injections at P15, analyses at ~P29). Input-output curves of fEPSP slope were strongly diminished in SIRP $\alpha^{-/-}$ mice relative to control littermates (Fig.

2f), whereas fiber volley amplitude (reflecting the number of axons firing to each stimulation) was unaffected, indicating that synaptic transmission is impaired in the absence of SIRP α .

Moreover, paired-pulse facilitation was dramatically increased in SIRP $\alpha^{-/-}$ mice relative to controls (Fig. 2g), suggesting that neurotransmitter release probability is diminished in the knockout mice. SIRP $\alpha^{-/-}$ neurons therefore have significant defects in excitatory presynaptic function. Taken together, the histological and electrophysiological results with SIRP $\alpha^{-/-}$ mice demonstrate that SIRP α is necessary for the maturation, but not induction or maintenance, of excitatory presynaptic terminals in the hippocampus *in vivo*.

Presynaptic maturation by SIRP α requires neural activity

During the maturation stage of synapse formation, activity-dependent signals either stabilize or destabilize the synapses to establish efficient synaptic connections. Therefore, we hypothesized that SIRP α contributes to mechanisms that stabilize and promote maturation of presynaptic terminals in response to neural activity.

To test this idea, we examined whether the presynaptic effects of SIRP α require neural activity. When SIRP α was transfected into cultured hippocampal neurons, the size of VGLUT1 puncta was significantly increased on the dendrites of SIRP α -expressing neurons relative to control (Fig. 3a,b). This SIRP α -dependent increase in VGLUT1 clustering was completely blocked by suppressing neural activity with the sodium channel blocker tetrodotoxin (TTX, 1 μ M) or by suppressing synaptic transmission with a cocktail of neurotransmitter receptor inhibitors (50 μ M APV, 10 μ M CNQX, 50 μ M bicuculline). These data suggest that neural activity is critical for SIRP α -dependent presynaptic maturation.

Neural activity cleaves the extracellular domain of SIRP α

What are the mechanisms by which neural activity controls SIRP α -dependent presynaptic maturation? A clue came from our initial identification of SIRP α as a presynaptic organizing molecule – the SIRP α protein we identified from the brain extract was the extracellular portion of SIRP α ¹⁶. In fact, from cultured neurons, we were able to collect secreted SIRP α in the media, and its molecular weight is smaller than full-length SIRP α expressed in neurons (Fig. 3c). In addition, we detected a short fragment of SIRP α containing its C-terminal domain (~16 Kd; size corresponding to the intracellular domain) in the synaptic membrane fraction (Supplementary Fig. 2). Therefore, we hypothesized that the extracellular domain of SIRP α is cleaved by neural activity, and that this cleavage is required for its presynaptic effects (see Supplementary Fig. 7a).

To examine whether the extracellular domain of SIRP α is cleaved and released from hippocampal neurons in response to neural activity, we cultured hippocampal cells with either KCl (50 mM) to depolarize neurons, bicuculline (50 μ M) to enhance endogenous network activity, or TTX (1 μ M) to suppress network activity. We then collected media and assessed the amount of cleaved and released SIRP α by immunoprecipitation followed by Western blot. KCl and bicuculline treatments significantly increased the amount of released SIRP α in media as compared to untreated control (Fig. 3d–f), while TTX treatment

significantly decreased the amount of cleaved SIRP α in the media, indicating that the SIRP α ectodomain is released by neural activation. These effects were not due to altered cell numbers, as the amount of tubulin in the cell lysate was not altered by any treatment condition. In addition, the amount of full-length SIRP α remaining on the cell was decreased in KCl-treated cultures, and increased in TTX-treated cultures (Fig. 3f,g), consistent with an increase or a decrease in SIRP α cleavage by KCl or TTX treatment, respectively.

Shedding of SIRP α is necessary for presynaptic maturation

We then investigated whether the cleavage of the extracellular domain of SIRP α is required for presynaptic maturation mediated by SIRP α . For this, we prepared a mutant form of SIRP α (MT-SIRP α) that is resistant to ectodomain shedding (Fig. 3h). In the HEK cell-hippocampal neuron co-culture system (see Fig. 1e), the number and size of synapsin puncta formed on HEK cells expressing MT-SIRP α were similar to those on control HEK cells (Fig. 3i), indicating that MT-SIRP α cannot promote synaptic vesicle clustering in hippocampal neurons.

We next transfected cultured hippocampal neurons with wild-type SIRP α (WT-SIRP α) or MT-SIRP α . The localization of MT-SIRP α was similar to that of WT-SIRP α (Supplementary Fig. 7b,c). Overexpression of WT-SIRP α led to an increase in the size of VGLUT1 puncta on the transfected neurons; however, overexpression of MT-SIRP α failed to do so (Fig. 3j). These results indicate that shedding-resistant SIRP α cannot promote presynaptic maturation both in co-culture and neuronal culture, suggesting that the cleavage and secretion of the SIRP α ectodomain are necessary for its presynaptic effects.

Neural activity is responsible for SIRP α cleavage

If neural activity is responsible for cleaving SIRP α , suppressing neural activity should inhibit the presynaptic effect of full-length SIRP α (Fig. 3a,b) but not that of soluble SIRP α (sSIRP α). To test this idea, we cultured hippocampal neurons with sSIRP α with or without TTX. Application of sSIRP α increased the size of VGLUT1 puncta, and unlike what was observed with full-length SIRP α , this effect was completely resistant to TTX (Fig. 3k). Thus, after cleavage, presynaptic maturation by SIRP α is no longer dependent on neural activity.

To exclude the possibility that SIRP α is subjected to constitutive cleavage in neurons followed by activity-dependent secretion of its cleaved product, we performed an experiment with a secretable form of SIRP α , which contains only the extracellular domain of SIRP α (Ext-SIRP α ; the construct used to prepare sSIRP α). When transfected into cultured neurons, Ext-SIRP α efficiently induced maturation of glutamatergic presynaptic terminals on the Ext-SIRP α expressing neurons (Fig. 3l). This presynaptic effect was not inhibited by TTX application, indicating that neural activity does not play important roles in the secretion of Ext-SIRP α . These results are consistent with the notion that neural activity is responsible for cleaving, and not secretion of, the extracellular domain of SIRP α .

CaMK and MMP mediate activity-dependent SIRP α cleavage

We further investigated the signaling pathway that is involved in activity-dependent SIRP α cleavage. CaMK is a major signaling molecule at synapses²⁷, prompting us to explore the possibility that CaMK contributes to SIRP α cleavage. Consistent with this hypothesis, treatment of hippocampal cultures with CaMK inhibitors, KN62 or KN93 (5 μ M), significantly decreased the amount of cleaved SIRP α in the media (Fig. 4a). We next examined the effects of a CaMK inhibitor (KN62) and a calcium channel blocker (nifedipine; 10 μ M) on activity-dependent cleavage of SIRP α . Both inhibitors suppressed KCl-induced SIRP α cleavage (Fig. 4b), suggesting that neural activity-dependent calcium entry followed by CaMK activation plays important roles in the ectodomain shedding of SIRP α .

We then characterized the proteases that cleave the extracellular domain of SIRP α . MMPs are zinc-dependent endopeptidases that cleave extracellular molecules and are implicated in synaptic function²⁸. We found that incubation of hippocampal neurons with MMP inhibitors, GM6001 (10 μ M) or TIMP (0.5 μ g/ml), markedly inhibited SIRP α shedding, including the augmented cleavage induced by KCl (Fig. 4c,d). These results suggest that calcium, CaMK, and MMP are involved in the activity-dependent shedding of SIRP α from hippocampal neurons.

CD47 is the presynaptic receptor for SIRP α

Since our data indicate that the shed SIRP α ectodomain promotes presynaptic maturation, we next examined the identity of its presynaptic receptor. We asked whether CD47, a receptor for SIRP α in hematopoietic cells^{18–20}, mediates the presynaptic effects of SIRP α . Immunostaining experiments showed that CD47 puncta were abundant in neurofilament-positive axons and not in MAP2-positive dendrites (Fig. 5a) and that CD47 co-localized with SIRP α (Fig. 5b), consistent with the idea that CD47 serves as a presynaptic receptor for SIRP α . We then used CD47^{-/-} neurons²⁹ to determine if CD47 mediates SIRP α 's effects. CD47^{-/-} neurons extended axons and dendrites normally (Supplementary Fig. 8), but did not increase the number and size of VGLUT1 puncta in response to sSIRP α application (Fig. 5c). The following two experiments suggest that CD47 acts as a presynaptic receptor for SIRP α : i) HEK cells expressing SIRP α , which can induce presynaptic differentiation in co-cultured WT hippocampal neurons, failed to do so in co-cultured CD47^{-/-} neurons; while neuroligin1 was able to induce presynaptic differentiation in both WT and CD47^{-/-} neurons (Fig. 5d), and ii) CD47^{-/-} neurons do not respond to sSIRP α application to induce presynaptic differentiation as assessed by synaptophysin-YFP clustering, but the responsiveness is restored by presynaptic expression of CD47 (Fig. 5e).

Finally, we confirmed that the source of SIRP α is postsynaptic: we found that presynaptic defects in SIRP α ^{-/-} neurons are rescued by postsynaptic expression of SIRP α (Fig. 5f). All together, these results strongly suggest that postsynaptic-derived SIRP α interacts with presynaptic CD47 to organize presynaptic maturation.

LTP is impaired in SIRP α ^{-/-} mice

What are the functional consequences of defects in SIRP α -dependent presynaptic maturation? To explore this question, we examined the impact of SIRP α -deficiency on activity-dependent synaptic plasticity in the hippocampus. We found that long-term potentiation (LTP) is impaired at CA3–CA1 synapses in the hippocampus of SIRP α ^{-/-} mice (Fig. 6); of relevance, CD47^{-/-} mice also show impaired LTP³⁰. This is consistent with the altered presynaptic function in SIRP α ^{-/-} mice (Fig. 2 and Supplementary Fig. 9) and demonstrates that SIRP α -dependent synapse maturation has an enduring impact on long-lasting forms of plasticity in hippocampal circuits.

DISCUSSION

Activity-dependent synapse maturation is a critical step for the refinement of neural circuits and the establishment of the appropriate and efficient synaptic map in the brain. However, little is known about the molecular mechanisms that control this important aspect of synapse development. Here, we have uncovered a new process by which neural activity contributes to synapse maturation. From our results, we propose that after initial synaptic differentiation by molecules such as FGF22¹⁷, synaptic activity regulates extracellular domain cleavage of postsynaptic SIRP α through CaMK and MMP, and the released SIRP α ectodomain, in turn, promotes the maturation of the presynaptic terminal through CD47 (Supplementary Fig. 7a). SIRP α -dependent synapse maturation has a significant impact on synaptic function and plasticity, as demonstrated by impaired basal transmission, diminished neurotransmitter release probability, and impaired LTP in SIRP α ^{-/-} mice.

To date, there are several molecules that are implicated in presynaptic development, including neuroligins, SynCAMs, ephrins/Ephs, LRRTMs, NGLs, FGFs, Wnts, neurotrophins, Cblns, and thrombospondins^{5–7,31–33}. Why are there multiple presynaptic organizers? We hypothesized that different presynaptic organizers are for the organization of different types of synapses (spatial specificity) and for the regulation of different stages of synapse formation (temporal specificity). As far as spatial specificity is concerned, we have previously shown that two FGFs, FGF22 and FGF7, are involved in the differentiation of two distinct types of synapses *in vivo*: FGF22 in excitatory and FGF7 in inhibitory¹⁷. Several presynaptic organizers such as neuroligin1, SynCAMs, Ephs, LRRTMs, and NGLs seem to be relatively specific to excitatory synapses, while others such as neuroligin2 and BDNF may be preferentially involved in inhibitory synapses. Thus, distinct presynaptic organizers indeed appear to be contributing to the organization of different synapses in the brain. As for temporal specificity, we here showed that in the hippocampus, FGF22 and SIRP α are important for two sequential stages of synapse formation, with FGF22 in initial synaptic differentiation and SIRP α in synapse maturation. Together, we propose that multiple spatially- and temporally-defined presynaptic organizers cooperate to organize specific and functional synaptic networks in the brain.

The role of SIRP α has been mainly studied in the immune system. Little is known about its function in the nervous system, but possible roles for SIRP α 's intracellular domain have been suggested: it promotes neurite outgrowth and enhances the effect of BDNF in culture^{20,34}, and mice expressing mutant SIRP α that lacks the intracellular domain show

prolonged immobility in the forced swim test³⁵. We focused on the role of SIRP α 's extracellular domain: using hippocampal cultures and conditional SIRP α knockout mice, we showed that the extracellular domain of SIRP α serves as a target-derived presynaptic organizer in the hippocampus and is critical in the maturation stage of synapse formation *in vitro* and *in vivo*. SIRP α 's extracellular domain is cleaved in response to neural activity, acting as an activity-dependent, target-derived presynaptic organizer. Why does SIRP α need to be cleaved for presynaptic maturation? Cleavage may be necessary for the extracellular domain of SIRP α to bind to its presynaptic receptor, CD47. Crystal structure models of SIRP α and CD47 suggest that the extracellular region of SIRP α -CD47 complex is ~14 nm^{36,37}. However, the cleft of excitatory synapses is ~25 nm, which may require the release of SIRP α ectodomain to bind to CD47. It will be also interesting to address the fate and roles of the SIRP α intracellular domain after cleavage.

Ectodomain shedding plays important roles in various processes including sperm-egg interaction, cell migration and adhesion, cell fate determination, wound healing, axon guidance, and immune responses³⁸⁻⁴⁰. Here we identified a novel role for ectodomain shedding: activity-dependent ectodomain shedding of SIRP α is involved in synapse maturation. Notably, while we were preparing our paper, two groups showed that activity-dependent cleavage of neuroligin1 is involved in synapse disassembly and negatively regulates synaptic function in a homeostatic manner^{41,42}. In contrast, our results demonstrate that activity-dependent cleavage of SIRP α is a critical positive regulator of synapse maturation during synapse development to establish functional circuits. It is also noteworthy that the cleavages of both SIRP α and neuroligin1 involve common pathways, CaMK and MMP; yet, they have opposite effects at synapses. Thus, our results, together with the neuroligin results, significantly expand the role of activity-dependent shedding in controlling synapse maturation and function. How activity-dependent shedding of SIRP α and neuroligin1 cooperate/antagonize to regulate synapses is an interesting next question to address. Finally, since defects in activity-dependent synapse maturation in the hippocampus have been implicated in various neurological and psychiatric disorders such as schizophrenia and autism¹⁻³, our results may help design strategies to prevent and treat such disorders.

ONLINE METHODS

In situ hybridization

In situ hybridization was performed as described⁴³ using digoxigenin-labeled riboprobes (Roche). The probes were generated by PCR from the 3' untranslated regions¹⁵⁻¹⁷.

Primary neuronal cultures and transfection

Hippocampal cultures were prepared as described¹⁷. For immunostaining, hippocampal cells (1.5×10^4 to 4×10^4) were plated on glass coverslips (diameter 12 mm) coated with poly-D-lysine. Transfection was performed using the CalPhos Mammalian transfection kit (Clontech). For immunoprecipitation, hippocampal cells (3×10^5 to 5×10^5) were plated on poly-D-lysine-coated tissue culture dishes (diameter 35 mm). For co-culture experiments, HEK cells were transfected using Lipofectamine 2000 (Invitrogen), and 24 hrs after

transfection, they were dissociated and added onto cultured hippocampal neurons (DIV 8). Co-cultures were maintained for 48 hrs before fixation.

Knockout and transgenic mice

SIRP α knockout mice: A *Sirpa* genomic clone containing exon 1 (BAC clone 394B7; Invitrogen) was used to construct a targeting vector. A gene cassette composed of floxed full-length mouse *Sirpa* cDNA with SV40 intron-poly(A), EGFP-poly(A), and FRTed Tn5 neo⁴⁴ was introduced into the first exon, deleting 71 nucleotides containing the start codon (Supplementary Fig. 5). The deletion disrupts the expression of the endogenous *Sirpa* gene but allows the expression of the inserted gene. Floxed SIRP α mice were generated by embryonic stem cell-based homologous recombination.

Actin-Cre-ER mice²⁵ were mated with floxed SIRP α mice. Tamoxifen (100 μ g to 1 mg) was injected at P0, P15, or P30 to induce the Cre recombinase-mediated excision of the *Sirpa* gene.

CD47 knockout mice²⁹ were from W. Frazier (Washington University).

Mice used were C57/BL6 background. Both male and female mice were used in our experiments. We did not detect any significant differences between males and females. All animal care and use was in accordance with the institutional guidelines and approved by the University Committee on Use and Care of Animals.

Immunohistochemistry

Cultures were fixed with methanol for 3 min at -20°C or with 1–4% paraformaldehyde (PFA) for 10 min at 37°C and stained as described¹⁷. Mouse brains were fixed for 24 hours with 4% PFA in PBS. Sagittal sections of 20 μm thickness were cut in a cryostat and stained. For immunostaining for PSD95, mouse brains were fresh-frozen and sectioned. Sections were then fixed with methanol for 5 min at -20°C and stained. Dilutions and sources of antibodies are: anti-VGLUT1 (1:5,000; Millipore; AB5905), anti-PSD95 (1:250; NeuroMab; 75-028), anti-VGAT (1:1,500; Synaptic Systems; 131003), anti-MAP2 (1:3,000; Sigma-Aldrich; M4403), anti-neurofilament (1:1,000; Covance; SMI-312), anti-bassoon (1:500; Enzo Life Sciences; ADI-VAM-PS003), anti-GFP (1:1,000; Millipore; AB16901), anti-GFAP (1:500; Synaptic Systems; 173002), anti-NeuN (1:500; Millipore; MAB377), anti-calbindin (1:500; Sigma; C9848), anti-synapsin (1:2000; a kind gift from P. Greengard and A. Nairn, Rockefeller University), antibody Py (1:50; a kind gift from M. Webb and P.L. Woodhams)⁴⁵, anti-CD47 (1:200; BD; miap301), polyclonal anti-SIRP α (against the SIRP α C-terminal domain; 1:200; Upstate Biotechnology; 06-729), and monoclonal anti-SIRP α (clone p84; 1:200; BD). Clone p84, which recognizes the extracellular domain of SIRP α and stains cell surface SIRP α , inhibits CD47-SIRP α interactions⁴⁶, suggesting that the epitope of this antibody may be close to the CD47 binding site of SIRP α , which is its most distal Ig domain³⁶.

Imaging and Quantification

Twelve-bit images at a resolution of $1,376 \times 1,032$ pixels were acquired on an Olympus BX61 epifluorescence microscope using $4\times$ ($2,226 \times 1,670 \mu\text{m}$ images), $10\times$ ($890 \times 668 \mu\text{m}$), $20\times$ ($444 \times 333 \mu\text{m}$), and $40\times$ ($221 \times 166 \mu\text{m}$) objective lenses and an F-View II CCD Camera (Soft Imaging System). Alternatively, twelve-bit images at a $1,024 \times 1,024$ pixel resolution were acquired on a confocal microscope (Olympus, FV1000) using $40\times$ objective lens with zoom $1.5\times$ ($211.8 \times 211.8 \mu\text{m}$). All images for each experiment were acquired with identical exposure time and detector gain.

For images of hippocampal sections stained for synaptic proteins, the average signal intensities of staining in the stratum lucidum and stratum radiatum layers were calculated with the MetaMorph software. The average signal intensity in the fimbria of the hippocampus was calculated and subtracted as the background. The intensity of the background was not significantly different between $\text{SIRP}\alpha^{-/-}$ and control mice. For images of cultured neurons stained for synaptic proteins, the staining intensity of the dendritic shaft was calculated and subtracted as the background. Puncta size and intensity were quantified using the MetaMorph or ImageJ software¹⁷.

Electron microscopy

P15 $\text{SIRP}\alpha$ conditional knockout mice and littermate controls were injected with tamoxifen. At P29, the mice were perfused transcardially with Karnovsky's fixative¹⁷. Hippocampi were removed, 1 mm cubes from the stratum radiatum layer of the CA3 region were dissected, and processed for electron microscopy. Thin sections (70 nm) were cut and observed with a Philips CM100 electron microscope at 60 kV. Digital images were captured with a Hamamatsu ORCA-HR digital camera system operated with Advanced Microscopy Techniques Corp. software.

Plasmid Constructs and Recombinant Proteins

A cDNA encoding mouse *Sirpa* (IMAGE: 5368250) was obtained from ATCC and cloned into the APTag5 expression vector (GenHunter) as described previously¹⁶. The mutant (shedding resistant) *Sirpa*^{A7} was generated by PCR using the following primers: 5'-GGATATCGATTACAAGGACGACGATGACAAGACCCACAACCTGGAATGTCTTCATCG-3' and 5'-AGGTATCGATATCCCCTTGATCACTCGAGTGG-3'. This replaced the juxtamembrane amino acids "SMQTFPGNNA" in the $\text{SIRP}\alpha$ protein with the FLAG epitope amino acids "DIDYKDDDDK".

The expression plasmid for FGF22 was described previously¹⁷. The expression plasmid for Neuroligin1 was from G. Rudenko (University of Michigan), CD47 (IMAGE: 4187965) was from Open Biosystems, and Cre was from D. Goldman (University of Michigan).

Soluble $\text{SIRP}\alpha$ proteins (s $\text{SIRP}\alpha$) were produced by transiently transfecting $\text{SIRP}\alpha$ extracellular-domain plasmids (= Ext- $\text{SIRP}\alpha$) into HEK cells and purifying secreted $\text{SIRP}\alpha$ proteins from culture media as described¹⁶. Recombinant FGF22 was from R&D Systems.

Immunoprecipitation

Hippocampal neurons were cultured for 10–12 days after which the media was replaced by new media (control), or media containing 50 mM KCl, 50 μ M bicuculline, 1 μ M TTX, 5 μ M KN62, 5 μ M KN93, 10 μ M nifedipine, 10 μ M GM6001, and/or 0.5 μ g/ml TIMP's (mixture of TIMP1 and TIMP2). After incubation for 1–3 days with these treatments, media and cells were collected. The media was precleared with Immobilized Protein-L (Pierce) and incubated with 1 μ g of anti-SIRP α extracellular domain antibody for 4 hrs at 4°C. The immune complexes were precipitated with Protein-L and the immunoprecipitates were subjected to Western blotting as described below to assess the amount of secreted SIRP α .

Western blotting

Cells, collected as described above, were lysed on ice for 1 hour in lysis buffer (1% Nonidet P-40, 50 mM Tris buffer, pH 8.0) with a protease inhibitor cocktail tablet (Roche). Dissected hippocampi were lysed by homogenization in lysis buffer containing 1% Triton, 50 mM Tris buffer (pH 7.4), and 150 mM NaCl with a protease inhibitor cocktail tablet. The immunoprecipitates and lysates were subjected to SDS-PAGE. Equal amounts of lysate from each group were applied to the gel, as confirmed by testing the level of α -tubulin. Proteins were transferred to a polyvinylidene fluoride (PVDF) membrane and probed using anti-SIRP α extracellular domain antibody (p84; 1:200; BD) and anti- α -tubulin antibody (1:5,000; Sigma; T6074). The proteins were visualized by chemiluminescence (GE Healthcare) and the band intensities were quantified with ImageJ software.

Synaptic protein fractionation

Fractionation protocol was adapted from a previous report⁴⁸. 300–350 mg of cortex from P21 mice was homogenized in 1.5 ml of homogenization buffer (0.32 M Sucrose, 1 mM NaHCO₃, 1 mM MgCl₂, 0.5 mM CaCl₂ and supplemented with protease inhibitor). Homogenate was then adjusted to 1.25 M Sucrose and 0.1 mM CaCl₂ to a total of 5 ml. Homogenate was overlaid on 5 ml of 1 M Sucrose and spun at 100,000g for 3 hours at 4°C. Interface was collected and designated as synaptic membrane fraction (SPM). 500 μ l of SPM was then added to 2 ml of 0.1 mM CaCl₂ and 2.5 ml of 40 mM Tris, pH 6 with 2% Triton X-100 and placed on rocking platform for 20 min at 4°C. Sample was then spun at 35,000g for 20 minutes at 4°C and supernatant was collected as extra-junctional fraction. Pellet was air dried and resuspended in 1 ml of 0.1 mM CaCl₂ and 1 ml of 40 mM Tris, pH 8 with 2% Triton X-100 and placed on rocking platform for 60 minutes. Resuspended pellets were then spun at 140,000g for 30 minutes at 4°C and supernatant was collected as presynaptic fraction. Insoluble fraction was resuspended in 1 ml 20 mM Tris pH 7.4 with 1% SDS and designated as postsynaptic fraction. Extra-junctional and presynaptic fractions were acetone precipitated and resuspended in 1 ml of 20 mM Tris pH 7.4 with 1% SDS. Synaptic membrane fraction and equivalent volumes of extra-junctional, presynaptic, and postsynaptic membrane fractions were then transferred to PVDF membrane and probed with anti-PSD95 antibody (1:500; NeuroMab; 75-028), anti-synaptotagmin antibody (1:100; Hybridoma Bank; mab48), and polyclonal anti-SIRP α antibody (1:500; Upstate; 06-729).

Whole-cell patch-clamp recordings in cultures

Neurons were bathed in HEPES buffered saline (HBS), containing 119 mM NaCl, 5 mM KCl, 2 mM CaCl₂, 2 mM MgCl₂, 30 mM glucose, and 10 mM HEPES (pH 7.4), supplemented with 1 μM TTX and 50 μM picrotoxin to isolate mEPSCs. Whole-cell internal solution included 100 mM gluconic acid, 0.2 mM EGTA, 5 mM MgCl₂, 2 mM ATP, 0.3 mM GTP, and 40 mM HEPES (pH 7.2). Recording pipettes had a resistance of 4–6 MΩ. Recordings were made with an Axopatch 200B amplifier and collected with Clampex 8.0 (Molecular Devices). mEPSCs were analyzed using Minianalysis 6.0 (Synaptosoft).

Acute hippocampal slice preparation and field electrophysiology

Mice were decapitated and the hippocampi were isolated. Transverse slices (400 μm) were cut using a tissue chopper (Stoelting) and incubated at 25°C in a humidified chamber for at least 2 hours before recording. Slices were then transferred to a recording chamber, maintained at 27–28°C and continuously perfused at rate of 1.5 ml/min with oxygenated artificial cerebral spinal fluid (aCSF). aCSF contained 119 mM NaCl, 2.5 mM KCl, 1 mM NaH₂PO₄, 26.3 mM NaHCO₃, 11 mM glucose, 1.3 mM MgSO₄, and 2.5 mM CaCl₂. In most experiments (except Fig. 6), aCSF also contained 50 μM picrotoxin during recording. Picrotoxin was perfused for at least 15 min before data were collected. Recording electrodes were pulled from borosilicate capillary glass (1.7 mm o.d.; VWR International), filled with 3M NaCl, and placed in the stratum radiatum layer of CA1. fEPSPs were stimulated using cluster electrodes (FHC) also placed in the stratum radiatum of CA1. Current was delivered with an ISO-flex stimulus isolation unit (AMPI). Recordings were made with a MultiClamp 700B amplifier, collected and analyzed using Clampfit 10.2 (Molecular Devices). An input output curve was obtained for each slice by increasing the stimulus intensity from 0.02 to 0.25 mA. For paired-pulse experiments, the intensity was set at 0.2 mA, which was the maximum response size. To obtain the paired-pulse ratio, two pulses were delivered with an inter-pulse interval from 25–200 ms. For LTP experiments, the stimulus intensity was set so that the response size was 50% of maximum, and test stimuli were delivered every 30 s. After 20 min of stable baseline fEPSPs, LTP was induced by delivering 4 trains (each 1-s in duration) of 100 Hz separated by 30-s each.

Statistical analysis

The statistical tests performed were two-tailed Student's t-test or Two-way ANOVA as indicated in the figure legend. In the case of a two-way ANOVA, post hoc analysis was done with Tukey's test. All data are expressed as mean ± SEM. Sample sizes were determined to ensure confidence in the results. No statistical methods were used to pre-determine sample sizes, but our sample sizes were similar to those reported in previous publications in the field^{15–17,41,42}. For all experiments, there was enough statistical power to detect the corresponding effect size. Data distribution was assumed to be normal, and in some cases, normality of the sample data was assessed graphically with QQ-plots. Apparent extreme values were excluded from analysis. These values were justified by the context: imaging artifacts, cell death, etc. All steps of the experiments were randomized to minimize the effects of confounding variables. This includes how mice were chosen for injections, order of cell culture treatments, etc. Electrophysiology experiments were done blind.

Imaging was done in similar fashions among conditions: fields from brain sections were chosen randomly from the region of interest, and images of cell cultures were taken randomly from all areas of the culture.

Supplementary Material

Refer to Web version on PubMed Central for supplementary material.

Acknowledgments

We thank J. Sanes for critical comments on the manuscript; H. Enomoto for pSV loxp sv40 intron polyA EGFP FRTneo plasmid; A. Murayama and L. Kee for plasmid construction; E. Gibbs for help with in situ hybridization; D. Sorenson for help with electron microscopy; M. Zhang, R. Carson, and A. Williams for technical assistance; E. Hughes, Y. Qu, K. Childs, G. Gavrilina, D. Vanheyningen and the Transgenic Animal Model Core of the University of Michigan for preparation of SIRPa knockout mice. Core support was provided by the University of Michigan Center for Organogenesis. This work was supported by the Ester A. & Joseph Klingenstein Fund, the Edward Mallinckrodt Jr. Foundation, the March of Dimes Foundation, the Whitehall Foundation, and NIH grants MH091429, NS070005, and MH092614 (H.U.).

References

1. Lipska BK, Halim ND, Segal PN, Weinberger DR. Effects of reversible inactivation of the neonatal ventral hippocampus on behavior in the adult rat. *J Neurosci.* 2002; 22:2835–2842. [PubMed: 11923448]
2. Pfeiffer BE, et al. Fragile X mental retardation protein is required for synapse elimination by the activity-dependent transcription factor MEF2. *Neuron.* 2010; 66:191–197. [PubMed: 20434996]
3. Kasai H, Fukuda M, Watanabe S, Hayashi-Takagi A, Noguchi J. Structural dynamics of dendritic spines in memory and cognition. *Trends Neurosci.* 2010; 33:121–129. [PubMed: 20138375]
4. Sanes JR, Lichtman JW. Development of the vertebrate neuromuscular junction. *Annu Rev Neurosci.* 1999; 22:389–442. [PubMed: 10202544]
5. Waites CL, Craig AM, Garner CC. Mechanisms of vertebrate synaptogenesis. *Annu Rev Neurosci.* 2005; 28:251–274. [PubMed: 16022596]
6. Fox MA, Umemori H. Seeking long-term relationship: axon and target communicate to organize presynaptic differentiation. *J Neurochem.* 2006; 97:1215–1231. [PubMed: 16638017]
7. Dalva MB, McClelland AC, Kayser MS. Cell adhesion molecules: signaling functions at the synapse. *Nat Rev Neurosci.* 2007; 8:206–220. [PubMed: 17299456]
8. Goda Y, Davis GW. Mechanisms of synapse assembly and disassembly. *Neuron.* 2003; 40:243–264. [PubMed: 14556707]
9. Tessier CR, Broadie K. Activity-dependent modulation of neural circuit synaptic connectivity. *Front Mol Neurosci.* 2009; 2:8. [PubMed: 19668708]
10. Kano M, Hashimoto K. Synapse elimination in the central nervous system. *Curr Opin Neurobiol.* 2009; 19:154–161. [PubMed: 19481442]
11. Zhang LI, Poo M. Electrical activity and development of neural circuits. *Nat Neurosci.* 2001; 4:1207–1214. [PubMed: 11687831]
12. Bleckert A, Wong RO. Identifying roles for neurotransmission in circuit assembly: insights gained from multiple model systems and experimental approaches. *Bioessays.* 2011; 33:61–72. [PubMed: 21110347]
13. Kay L, Humphreys L, Eickholt BJ, Burrone J. Neuronal activity drives matching of pre- and postsynaptic function during synapse maturation. *Nat Neurosci.* 2011; 14:688–690. [PubMed: 21532580]
14. Flavell SW, Greenberg ME. Signaling mechanisms linking neuronal activity to gene expression and plasticity of the nervous system. *Annu Rev Neurosci.* 2008; 31:563–590. [PubMed: 18558867]

15. Umemori H, Linhoff MW, Onitz DM, Sanes JR. FGF22 and its close relatives are presynaptic organizing molecules in the mammalian brain. *Cell*. 2004; 118:257–270. [PubMed: 15260994]
16. Umemori H, Sanes JR. Signal regulatory proteins (SIRPs) are secreted presynaptic organizing molecules. *J Biol Chem*. 2008; 283:34053–34061. [PubMed: 18819922]
17. Terauchi A, Johnson-Venkatesh EM, Toth AB, Javed D, Sutton MA, Umemori H. Distinct FGFs promote differentiation of excitatory and inhibitory synapses. *Nature*. 2010; 465:783–787. [PubMed: 20505669]
18. van Beek EM, Cochrane F, Barclay AN, van den Berg TK. Signal regulatory proteins in the immune system. *J Immunol*. 2005; 175:7781–7787. [PubMed: 16339510]
19. Barclay AN, Brown MH. The SIRP family of receptors and immune regulation. *Nat Rev Immunol*. 2006; 6:457–464. [PubMed: 16691243]
20. Matozaki T, Murata Y, Okazawa H, Ohnishi H. Functions and molecular mechanisms of the CD47-SIRP α signaling pathway. *Trends Cell Biol*. 2009; 19:72–80. [PubMed: 19144521]
21. Danglot L, Triller A, Marty S. The development of hippocampal interneurons in rodents. *Hippocampus*. 2006; 16:1032–1060. [PubMed: 17094147]
22. Steward O, Falk PM. Selective localization of polyribosomes beneath developing synapses: a quantitative analysis of the relationships between polyribosomes and developing synapses in the hippocampus and dentate gyrus. *J Comp Neurol*. 1991; 314:545–557. [PubMed: 1814974]
23. Bouvier D, Corera AT, Tremblay ME, Riad M, Chagnon M, Murai KK, Pasquale EB, Fon EA, Doucet G. Pre-synaptic and post-synaptic localization of EphA4 and EphB2 in adult mouse forebrain. *J Neurochem*. 2008; 106:682–695. [PubMed: 18410519]
24. Biederer T, Scheiffele P. Mixed-culture assays for analyzing neuronal synapse formation. *Nat Protoc*. 2007; 2:670–676. [PubMed: 17406629]
25. Guo C, Yang W, Lobe CG. A Cre recombinase transgene with mosaic, widespread tamoxifen-inducible action. *Genesis*. 2002; 32:8–18. [PubMed: 11835669]
26. Yasuda M, Johnson-Venkatesh EM, Zhang H, Parent JM, Sutton MA, Umemori H. Multiple forms of activity-dependent competition refine hippocampal circuits in vivo. *Neuron*. 2011; 70:1128–1142. [PubMed: 21689599]
27. Wayman GA, Lee YS, Tokumitsu H, Silva AJ, Soderling TR. Calmodulin-kinases: modulators of neuronal development and plasticity. *Neuron*. 2008; 59:914–931. [PubMed: 18817731]
28. Ethell IM, Ethell DW. Matrix metalloproteinases in brain development and remodeling: synaptic functions and targets. *J Neurosci Res*. 2007:2813–2823. [PubMed: 17387691]
29. Lindberg FP, Bullard DC, Caver TE, Gresham HD, Beaudet AL, Brown EJ. Decreased resistance to bacterial infection and granulocyte defects in IAP-deficient mice. *Science*. 1996; 274:795–798. [PubMed: 8864123]
30. Chang HP, Lindberg FP, Wang HL, Huang AM, Lee EH. Impaired memory retention and decreased long-term potentiation in integrin-associated protein-deficient mice. *Learn Mem*. 1999:448–457. [PubMed: 10541465]
31. Shen K, Cowan CW. Guidance molecules in synapse formation and plasticity. *Cold Spring Harb Perspect Biol*. 2010; 2(4):a001842. [PubMed: 20452946]
32. Williams ME, de Wit J, Ghosh A. Molecular mechanisms of synaptic specificity in developing neural circuits. *Neuron*. 2010; 68:9–18. [PubMed: 20920787]
33. Siddiqui TJ, Craig AM. Synaptic organizing complexes. *Curr Opin Neurobiol*. 2011; 21:132–143. [PubMed: 20832286]
34. Wang XX, Pfenninger KH. Functional analysis of SIRP α in the growth cone. *J Cell Sci*. 2006; 119:172–183. [PubMed: 16371655]
35. Ohnishi H, et al. Stress-evoked tyrosine phosphorylation of signal regulatory protein α regulates behavioral immobility in the forced swim test. *J Neurosci*. 2010; 30:10472–10483. [PubMed: 20685990]
36. Hatherley D, et al. Paired receptor specificity explained by structures of signal regulatory proteins alone and complexed with CD47. *Mol Cell*. 2008; 31:266–277. [PubMed: 18657508]

37. Hatherley D, Graham SC, Harlos K, Stuart DI, Barclay AN. Structure of signal-regulatory protein α : a link to antigen receptor evolution. *J Biol Chem*. 2009; 284:26613–26619. [PubMed: 19628875]
38. Edwards DR, Handsley MM, Pennington CJ. The ADAM metalloproteinases. *Mol Aspects Med*. 2008; 29:258–289. [PubMed: 18762209]
39. Reiss K, Saftig P. The “a disintegrin and metalloprotease” (ADAM) family of sheddases: physiological and cellular functions. *Semin Cell Dev Biol*. 2009; 20:126–137. [PubMed: 19049889]
40. Bai G, Pfaff SL. Protease Regulation: The Yin and Yang of Neural Development and Disease. *Neuron*. 2011; 72:9–21. [PubMed: 21982365]
41. Peixoto RT, et al. Transsynaptic signaling by activity-dependent cleavage of neuroligin-1. *Neuron*. 2012; 76:396–409. [PubMed: 23083741]
42. Suzuki K, et al. Activity-dependent proteolytic cleavage of neuroligin-1. *Neuron*. 2012; 76:410–22. [PubMed: 23083742]
43. Schaeren-Wiemers N, Gerfin-Moser A. A single protocol to detect transcripts of various types and expression levels in neural tissue and cultured cells: in situ hybridization using digoxigenin-labelled cRNA probes. *Histochemistry*. 1993; 100:431–440. [PubMed: 7512949]
44. Uesaka T, et al. Conditional ablation of GFR α 1 in postmigratory enteric neurons triggers unconventional neuronal death in the colon and causes a Hirschsprung’s disease phenotype. *Development*. 2007; 134:2171–2181. [PubMed: 17507417]
45. Woodhams PL, Webb M, Atkinson DJ, Seeley PJ. A monoclonal antibody, Py, distinguishes different classes of hippocampal neurons. *J Neurosci*. 1989; 9:2170–2181. [PubMed: 2470877]
46. Oldenborg PA, Zheleznyak A, Fang YF, Lagenaur CF, Gresham HD, Lindberg FP. Role of CD47 as a marker of self on red blood cells. *Science*. 2000; 288:2051–4. [PubMed: 10856220]
47. Ohnishi H, et al. Ectodomain shedding of SHPS-1 and its role in regulation of cell migration. *J Biol Chem*. 2004; 279:27878–27887. [PubMed: 15123722]
48. Hahn CG, et al. The post-synaptic density of human postmortem brain tissues: an experimental study paradigm for neuropsychiatric illnesses. *PLoS One*. 2009; 4(4):e5251. [PubMed: 19370153]

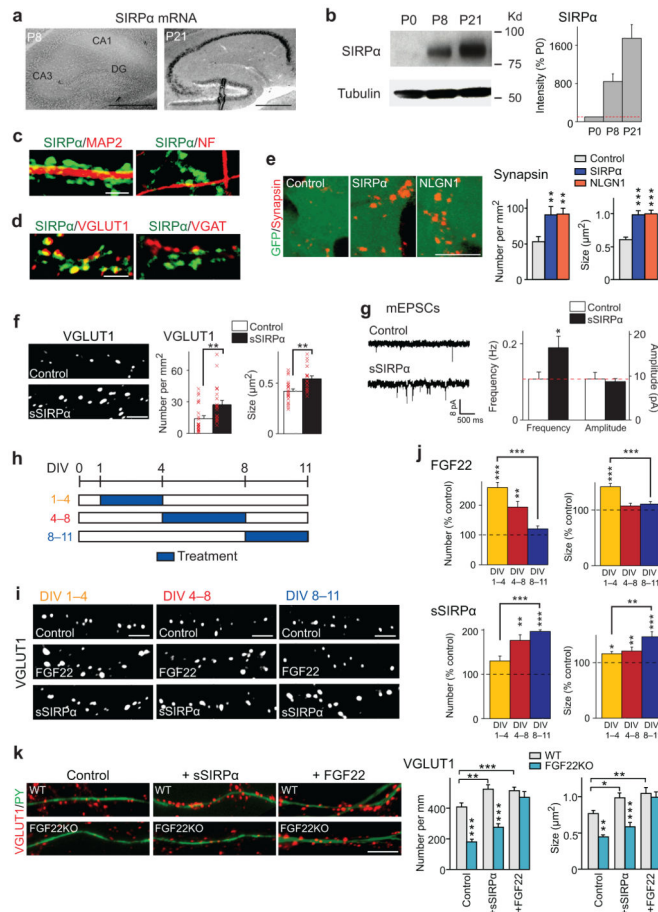


Figure 1. FGF22 and SIRP α promote the early or late stage of glutamatergic presynaptic differentiation

(a) *In situ* hybridization for *Sirpa* in the hippocampus during synapse formation (positive signals in black). *Sirpa* mRNA is highly expressed at P21, the time for synapse maturation, but not at P8, the time for initial synapse differentiation. Reproduced three times.

(b) Western blotting for the SIRP α protein (tubulin as control) in the hippocampus. The amount of SIRP α significantly increases from P8 to P21. Full-length blots are presented in Supplementary Figure 10.

(c,d) Hippocampal cultures at DIV11 were stained with the antibodies indicated. (c) SIRP α proteins are abundant on MAP2-positive dendrites but not on neurofilament (NF)-positive axons. (d) SIRP α is concentrated at VGLUT1-positive glutamatergic synapses but not at VGAT-positive GABAergic synapses. Reproduced five times.

(e) HEK cells expressing SIRP α , neuroligin1 (NLGN1), or control HEK cells (labeled with GFP) were co-cultured with hippocampal neurons for 2 days and stained for synapsin. The synapsin puncta formed on HEK cells expressing SIRP α are significantly more dense and larger than those formed on control HEK cells and are comparable to the ones on HEK cells expressing NLGN1. Data are from 24/23/22 fields from 5 cultures.

(f,g) Recombinant soluble SIRP α (sSIRP α) was applied to hippocampal cultures from DIV1–11. (f) sSIRP α treatment significantly increases the number (x 1,000 puncta per mm²) and size of VGLUT1 puncta as compared to PBS control (n = 57 fields from 5 cultures). (g)

Representative traces and summary data of whole-cell recordings of mEPSCs from control and sSIRP α -treated hippocampal neurons. mEPSC frequency, but not amplitude, increases by sSIRP α treatment. (n = 57/63 cells from 5 cultures).

(h) Schematic timeline of the experiment shown in (i,j). Cultured hippocampal cells were treated with FGF22 or sSIRP α from DIV1–4 (beginning of synapse formation), DIV4–8 (middle of synapse formation), or DIV8–11 (ending of synapse formation). All cultures were fixed on DIV11.

(i) Staining of hippocampal cultures for VGLUT1 after treatment with FGF22 or sSIRP α as shown in (h).

(j) Numbers and sizes of VGLUT1 puncta after treatment on DIV1–4, DIV4–8, or DIV8–11. FGF22 treatment is most effective at increasing VGLUT1 clustering when incubated from DIV1–4, while sSIRP α is most effective when incubated from DIV8–11. Data are shown as percentage of PBS control and from 32/43/40/34/27/26 fields from 5 cultures.

(k) sSIRP α or FGF22 was applied to hippocampal cultures prepared from WT or FGF22KO mice, and the cultures were stained for VGLUT1 and Py, which labels dendrites of CA3 pyramidal neurons. Fewer and smaller VGLUT1 puncta were on CA3 neurons in FGF22KO cultures relative to WT cultures; the defects were rescued by the application of FGF22, but not by sSIRP α . n = 19/23/25/25/17/23 neurites from 3 cultures.

Bars in the graphs are mean \pm SEM. *p < 0.05, **p < 0.01, ***p < 0.0001 (here and in subsequent figures) by Student's t-test (f,g) or by ANOVA followed by Tukey test (e,j,k). Scale bars, 500 μ m (a), 10 μ m (e,k), and 5 μ m (others).

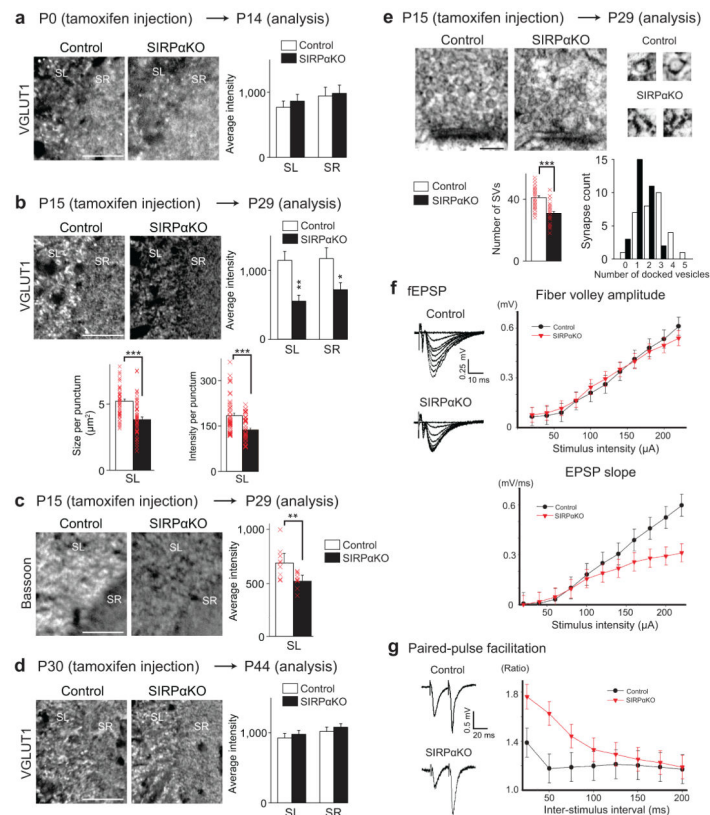


Figure 2. SIRP α is required for the maturation, but not induction or maintenance, of excitatory presynaptic terminals in the hippocampus *in vivo*

(a–d) SIRP α was inactivated around the time of initial synapse differentiation (P0–P14; a), synapse maturation (P15–P29; b,c), or synapse maintenance (P30–P44; d) by tamoxifen injections into conditional SIRP α KO mice. Control animals also received tamoxifen. Hippocampal sections from the control and SIRP α KO mice were stained for VGLUT1 (a,b,d) or bassoon (c). Images are from CA3 (positive signals in white). SL, stratum lucidum; SR, stratum radiatum. Graphs show the measurements of the relative intensity of VGLUT1 or bassoon staining (% control). (a) Mice were injected with tamoxifen at P0 and analyzed at P14. No significant difference in the VGLUT1 staining intensity between control and SIRP α KO at this time period. (b,c) Mice were injected with tamoxifen at P15 and analyzed at P29. The VGLUT1 (b) and bassoon (c) staining intensities are significantly decreased in SIRP α KO mice relative to control. Quantifications of the average size and intensity of VGLUT1 puncta are also shown in (b). (d) Mice were injected with tamoxifen at P30 and analyzed at P44. No significant difference between control and SIRP α KO at this time period. Staining data are from 12/20 sections from 3/5 mice. (e) Electron microscopic analysis of asymmetric (excitatory) synapses in CA3 of P29 mice injected with tamoxifen at P15. High magnification views of synaptic vesicles (SVs) are shown on the right. The numbers of SVs within 400 nm of the active zone and the numbers of docked vesicles are quantified. Significantly fewer SVs and docked vesicles are found in asymmetric synapses in SIRP α KO mice relative to control. Data are from 30 synapses from 3 mice. Student's t-test (a–e). Scale bars, 50 μ m (a) and 100 nm (e).

(f) Evoked fEPSPs were recorded in acute slices from CA1 of SIRP α KO mice and control littermates (tamoxifen injections at P15, analyses at P29). Sample traces of fEPSP recordings are shown. In input-output curves (right), fEPSP slope, but not fiber volley amplitude, is significantly decreased in SIRP α KO mice relative to control littermates ($p < 0.001$ by two-way ANOVA; $n = 9/13$ cells from 4 mice).

(g) Paired-pulse facilitation (PPF) across a range of inter-stimulus intervals for evoked EPSCs from SIRP α KO mice and control littermates. PPF is significantly enhanced in SIRP α KO mice ($p < 0.001$ by two-way ANOVA; $n = 11/15$ cells from 4 mice).

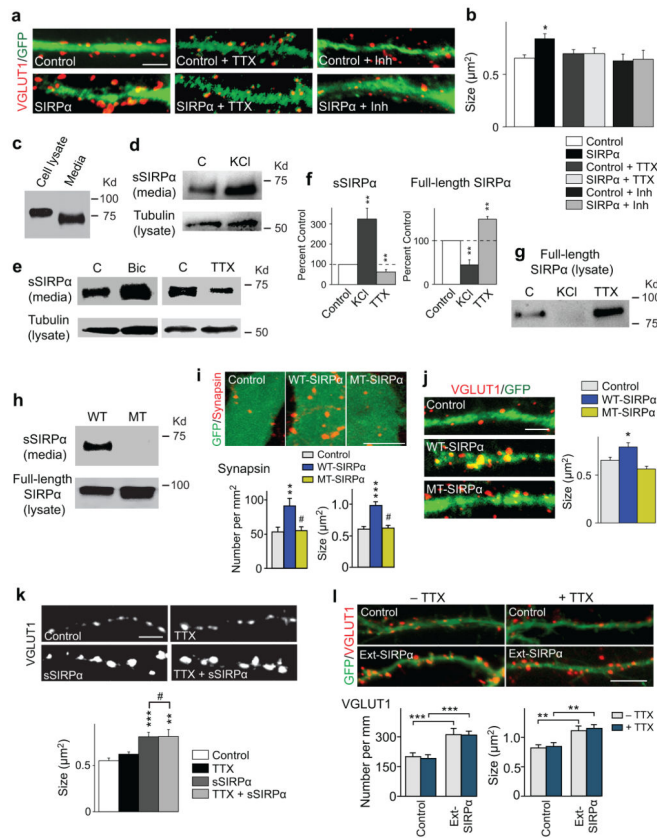


Figure 3. Cleavage of the extracellular domain of SIRP α is activity-dependent and is necessary for SIRP α -dependent presynaptic maturation

(a,b) Hippocampal neurons were transfected with a GFP plasmid (Control) or SIRP α and GFP plasmids (SIRP α) at DIV4. TTX or a cocktail of inhibitors for neurotransmitter receptors (APV, CNQX, bicuculline) was applied from DIV5. Cultures were stained for VGLUT1 on DIV13. VGLUT1 clustering on the dendrites of SIRP α -transfected neurons is increased in size as compared to control, but addition of TTX or the inhibitor cocktail prevents this increase. $n = 10$ neurites from 3 cultures.

(c) Hippocampal neurons were cultured for 11 days. Media and cell lysates were assayed for SIRP α . Reproduced five times.

(d–g) Hippocampal neurons were cultured for 10–12 days and then incubated with KCl, bicuculline, or TTX for 1–3 days. Media was collected and assayed for the amount of secreted SIRP α (sSIRP α) by immunoprecipitation followed by Western blotting (d,e). Cell lysates were also prepared and assayed for tubulin (d,e) and full-length SIRP α remaining on the cell (g) by Western blotting. In all conditions tested, tubulin levels are similar among the cell lysates. (d) Addition of KCl to activate neurons increases the amount of secreted SIRP α in the media as compared to control. (e) Bicuculline increases the amount of sSIRP α in the media, while TTX decreases it. (f) Quantification of the band intensity from results such as those shown in (d,e,g). Intensities were normalized against the intensity of the control band. $n = 5/3$ blots from 5/3 cultures. (g) In the cell lysate, the amount of full-length SIRP α is decreased in KCl-treated cultures and increased in TTX-treated cultures.

(h) Verification of cleavage-resistant mutant SIRP α . HEK cells were transfected with the wild-type SIRP α or cleavage-resistant mutant SIRP α (MT) plasmid for 2 days. Media and cell lysates were assayed for sSIRP α or full-length SIRP α . MT-SIRP α shows no release of sSIRP α . Reproduced three times.

(i) HEK cells expressing WT- or MT-SIRP α and control HEK cells (labeled with GFP) were co-cultured with hippocampal neurons for 2 days and stained for synapsin. MT-SIRP α does not increase the number and size of synapsin puncta. Data are from 24/24/33 fields from at 5 cultures.

(j) Hippocampal neurons were transfected with the GFP plasmid (Control) or the WT- or MT-SIRP α plasmid together with the GFP plasmid at DIV4 and stained for VGLUT1 at DIV13. VGLUT1 puncta on the dendrites of WT-SIRP α -transfected neurons, but not on those of MT-SIRP α -transfected neurons, are increased in size as compared to control. n = 23 neurites from 3 cultures.

(k) Presynaptic maturation induced by soluble SIRP α is not dependent on neural activity. Hippocampal neurons were treated with a bath application of sSIRP α and/or TTX from DIV1, and stained for VGLUT1 at DIV13. sSIRP α increases the size of VGLUT1 puncta, and adding TTX has no effect on the VGLUT1 clustering induced by sSIRP α . n = 13 fields from 3 cultures.

(l) Hippocampal neurons were transfected with the GFP plasmid (Control) or the Ext-SIRP α and GFP plasmids (Ext-SIRP α = secretable SIRP α) at DIV4. TTX was applied from DIV5. Cultures were stained for VGLUT1 on DIV13. VGLUT1 clustering on the dendrites of Ext-SIRP α -transfected neurons is increased in number and size as compared to control, and addition of TTX has no effect on this increase. n = 26/23/21/24 neurites from 3 cultures.

Student's t-test (b,f) or ANOVA followed by Tukey test (i-l). #: not significant. Scale bars, 10 μ m (i,l), 5 μ m (a,j,k).

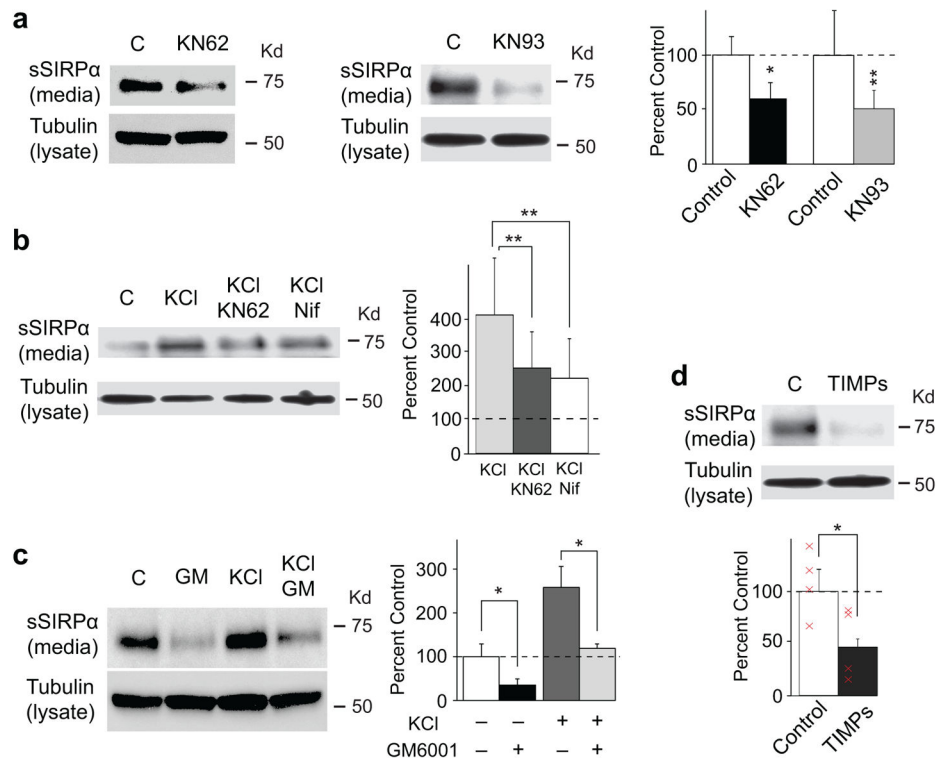


Figure 4. SIRP α -dependent presynaptic maturation involves calcium channel, CaMK, and MMP (a–d) Hippocampal neurons were cultured for 10–12 days and then incubated with a calcium channel blocker - nifedipine, CaMK inhibitors - KN62 or KN93, or MMP inhibitors - GM6001 or TIMPs, in the presence or absence of KCl for 1–3 days. Media was collected and assayed for the amount of secreted SIRP α . Cell lysates were assayed for tubulin. Quantification of the sSIRP α band intensity is shown in the graphs (normalized against control). Nifedipine, KN62, KN93, GM6001, and TIMPs effectively decrease the amount of sSIRP α found in the media (Student's t-test). $n = 4$ blots from 4 cultures.

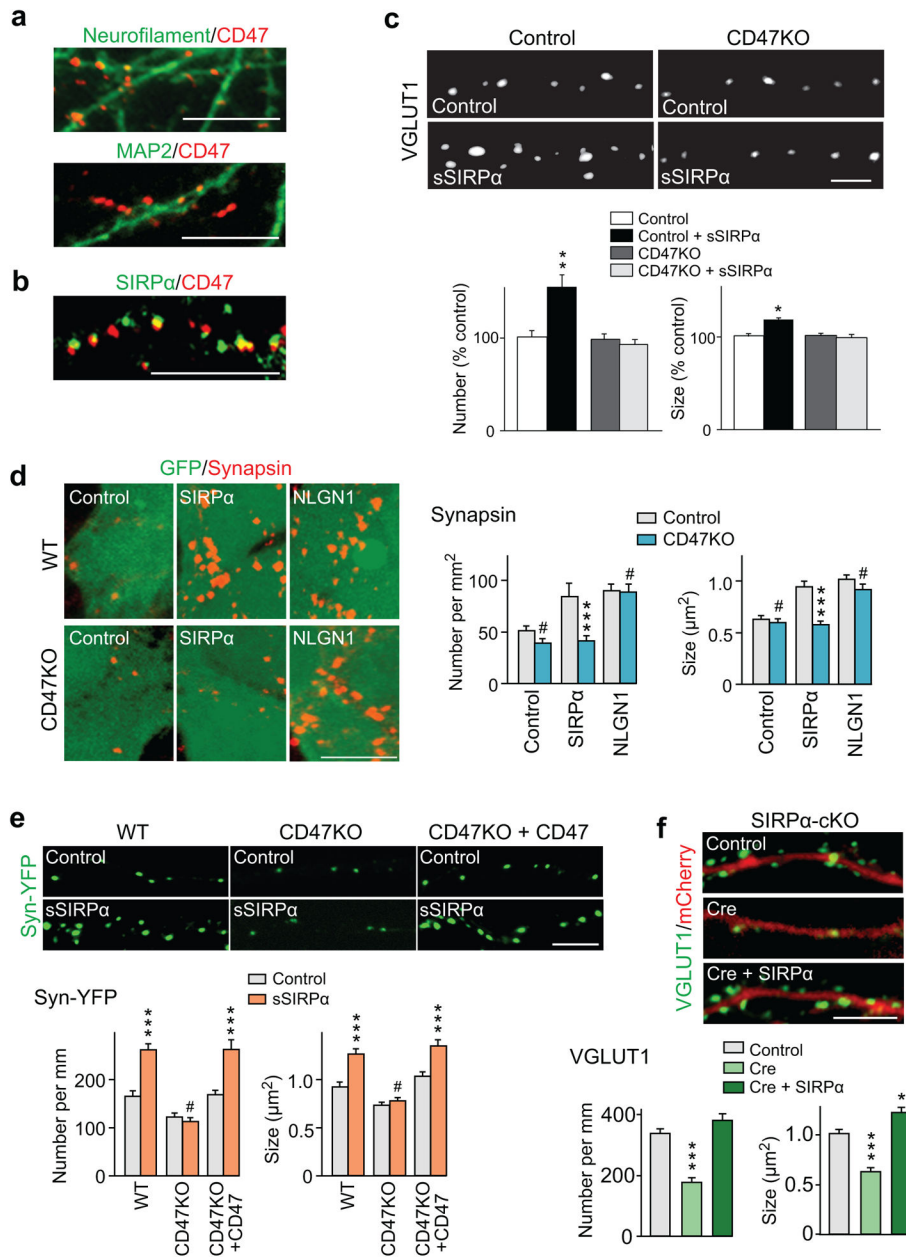


Figure 5. CD47 is the presynaptic receptor for SIRP α -mediated presynaptic maturation
 (a,b) Hippocampal neurons were stained for CD47 together with neurofilament, MAP2 or SIRP α . CD47 puncta are abundant in neurofilament-positive axons and not in MAP2-positive dendrites (a) and co-localized with SIRP α (b). Reproduced five times.
 (c) Hippocampal neurons prepared from CD47KO mice and control littermates were treated with sSIRP α and stained for VGLUT1. sSIRP α does not increase the number and size of VGLUT1 puncta in CD47KO neurons. $n = 80/93/102/108$ fields from 4 cultures.
 (d) HEK cells expressing SIRP α , neuroligin1, or control HEK cells (labeled with GFP) were co-cultured with hippocampal neurons prepared from WT or CD47KO mice for 2 days and stained for synapsin. HEK cells expressing SIRP α induce presynaptic differentiation in co-cultured WT hippocampal neurons, but fail to do so in co-cultured CD47KO neurons. HEK

cells expressing neuroligin1 induce presynaptic differentiation in both WT and CD47KO neurons. Graphs show quantification of synapsin puncta number and size. Data are from 38/34/34/35/42/40 fields from 5 cultures.

(e) Presynaptic expression of CD47 restores responsiveness to sSIRP α in CD47KO neurons. Hippocampal neurons prepared from WT or CD47KO mice were transfected with the synaptophysin-YFP plasmid or with the synaptophysin-YFP and CD47 plasmids. Cultures were treated with sSIRP α , and presynaptic differentiation of transfected neurons was assessed by synaptophysin-YFP clustering. sSIRP α does not increase the number and size of synaptophysin-YFP puncta in CD47KO neurons, but introduction of CD47 restores responsiveness to sSIRP α . n = 33/37/33/35/37/36 neurites from 3 cultures.

(f) Postsynaptic expression of SIRP α rescues presynaptic defects in SIRP α KO neurons. Hippocampal neurons prepared from conditional SIRP α KO mice were transfected with an mCherry plasmid (control), Cre and mCherry plasmids (knockout) or Cre, mCherry and SIRP α plasmids (rescue) and stained for VGLUT1. Both the number and size of VGLUT1 puncta on mCherry-expressing dendrites were decreased in SIRP α KO relative to control, but postsynaptic expression of SIRP α rescues the defects. n = 41/33/36 neurites from 3 cultures.

Student's t-test (c) or ANOVA followed by Tukey test (d-f). Scale bar, 5 μ m (c), 10 μ m (all others).

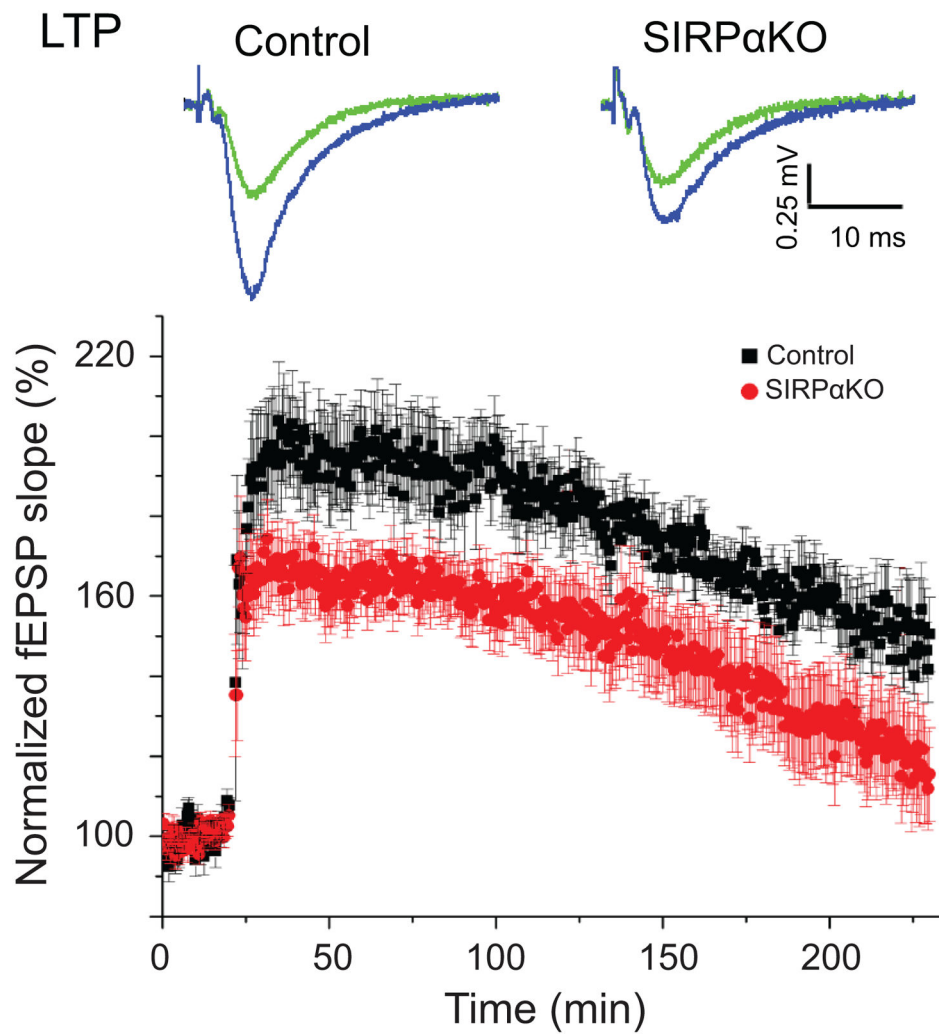


Figure 6. Impact of SIRP α -dependent presynaptic maturation on synaptic plasticity
Hippocampal slices were prepared from SIRP α KO mice and control littermates and fEPSPs recorded at CA3–CA1 synapses. LTP was induced by high frequency stimulation (four trains of 1s, 100 Hz stimulations spaced by 30s intervals). LTP is significantly impaired in SIRP α KO mice ($p < 0.05$ by Student's t-test at 1 hour after the LTP induction). $n = 20/10$ slices from 11/7 mice.